Atmospheric Research 168 (2016) 33–48

Contents lists available at ScienceDirect

Atmospheric Research

journal homepage: www.elsevier.com/locate/atmos

Changes in extreme temperature and precipitation events in the Loess Plateau (China) during 1960–2013 under global warming

Wenyi Sun [a], Xingmin Mu [a], Xiaoyan Song [b,*], Dan Wu [c], Aifang Cheng [d], Bing Qiu [e]

[a] Institute of Soil and Water Conservation, Northwest A&F University, Yangling 712100, Shaanxi, China
[b] College of Water Resources and Architectural Engineering, Northwest A&F University, Yangling 712100, Shaanxi, China
[c] Nanjing Institute of Environmental Sciences, Ministry of Environmental Protection, Nanjing 210042, China
[d] Key Laboratory of Disaster Monitoring and Mechanism Simulating of Shaanxi Province, Baoji University of Arts and Sciences, Baoji 721013, Shaanxi, China
[e] General Institute of Water Resources and Hydropower Planning and Design, Ministry of Water Resources, Beijing 100120, China

ARTICLE INFO

Article history:
Received 13 April 2015
Received in revised form 31 August 2015
Accepted 2 September 2015
Available online 5 September 2015

Keywords:
Extreme climatic events
Temperature
Precipitation
The Loess Plateau in China
Large-scale atmospheric circulation

ABSTRACT

In recent decades, extreme climatic events have been a major issue worldwide. Regional assessments on various climates and geographic regions are needed for understanding uncertainties in extreme events' responses to global warming. The objective of this study was to assess the annual and decadal trends in 12 extreme temperature and 10 extreme precipitation indices in terms of intensity, frequency, and duration over the Loess Plateau during 1960–2013. The results indicated that the regionally averaged trends in temperature extremes were consistent with global warming. The occurrence of warm extremes, including summer days (SU), tropical nights (TR), warm days (TX90), and nights (TN90) and a warm spell duration indicator (WSDI), increased by 2.76 ($P < 0.01$), 1.24 ($P < 0.01$), 2.60 ($P = 0.0003$), 3.41 ($P < 0.01$), and 0.68 ($P = 0.0041$) days/decade during the period of 1960–2013, particularly, sharp increases in these indices occurred in 1985–2000. Over the same period, the occurrence of cold extremes, including frost days (FD), ice days (ID), cold days (TX10) and nights (TN10), and a cold spell duration indicator (CSDI) exhibited decreases of −3.22 ($P < 0.01$), −2.21 ($P = 0.0028$), −2.71 ($P = 0.0028$), −4.31 ($P < 0.01$), and −0.69 ($P = 0.0951$) days/decade, respectively. Moreover, extreme warm events in most regions tended to increase while cold indices tended to decrease in the Loess Plateau, but the trend magnitudes of cold extremes were greater than those of warm extremes. The growing season (GSL) in the Loess Plateau was lengthened at a rate of 3.16 days/decade ($P < 0.01$). Diurnal temperature range (DTR) declined at a rate of −0.06 °C /decade ($P = 0.0931$). Regarding the precipitation indices, the annual total precipitation (PRCPTOT) showed no obvious trends ($P = 0.7828$). The regionally averaged daily rainfall intensity (SDII) exhibited significant decreases (−0.14 mm/day/decade, $P = 0.0158$), whereas consecutive dry days (CDD) significantly increased (1.96 days/decade, $P = 0.0001$) during 1960–2013. Most of stations with significant changes in SDII and CDD occurred in central and southeastern Loess Plateau. However, the changes in days of erosive rainfall, heavy rain, rainstorm, maximum 5-day precipitation, and very-wet-day and extremely wet-day precipitation were not significant. Large-scale atmospheric circulation indices, such as the Western Pacific Subtropical High Intensity Index (WPSHII) and Arctic Oscillation (AO), strongly influences warm/cold extremes and contributes significantly to climate changes in the Loess Plateau. The enhanced geopotential height over the Eurasian continent and increase in water vapor divergence in the rainy season have contributed to the changes of the rapid warming and consecutive drying in the Loess Plateau.

1. Introduction

Extreme weather and climatic events in recent decades have been a worldwide issue due to their potentially severe impacts on human life, the economy, and natural ecosystems (Aguilar et al., 2009; Rosenzweig et al., 2001; Zwiers et al., 2013). The Fourth Assessment Report (AR4) of the Intergovernmental Panel on Climate Change (IPCC, 2007) noted that hot days and warm nights were very likely to increase for over 70% of the global land area. Furthermore, cool days and nights are likely to decrease, heavy precipitation events in many mid-latitude regions are likely to increase, and the total area affected by drought since the 1970s has likely increased (Alexander et al., 2006; IPCC, 2007). These results show that the global climate is undergoing a significant change, which is mainly manifested as a warming trend. This warming not only directly influences the changes in temperature extremes but also enhances the frequency and intensity of extreme climate events, such as high temperatures, droughts, rainstorms, and floods (Kunkel et al., 1999a; H. Wang et al., 2012). Extreme events are

* Corresponding author at: Xinong Road 26, Yangling, Shaanxi 712100, China. Tel.: +86 29 87012411; fax: +86 29 87012210.
E-mail address: songxiaoyan107@mails.ucas.ac.cn (X. Song).

http://dx.doi.org/10.1016/j.atmosres.2015.09.001
0169-8095/

relatively rare, unpredictable, and often brief, but they are highly destructive to economically important agriculture and natural ecosystems (Kharin et al., 2007; Marengo et al., 2009); to some degree, extreme event occurrences have a far greater impact than the cited risks of global warming (Fankhauser, 1995; Meehl et al., 2000). Many studies show that climate extremes cause significant damage to crop growth and final yields, and the various frequencies and intensities of extreme events result in differing degrees of soil erosion and flooding (Li et al., 2009; Mu et al., 2007). The frequency of extreme events is likely to increase in the future. To predict future change in extremes, understanding the recent past is essential.

Climate changes have varying impacts on geographically diverse regions. As a result, the changes in extreme events show large regional variations (Liu et al., 2013; Ren et al., 2011). For example, a 50 mm daily precipitation is considered "normal" in rain-rich regions in Southeast China but is an "extreme" event in arid or semi-arid areas in Northwest China (Xin et al., 2011; Xu et al., 2011). A few heavy rainfall events often account for the total soil loss at a location in ecologically fragile areas, such as the Loess Plateau, but do not generate much sediment in densely vegetated areas (Ouyang et al., 2010). Similar studies have been conducted in many regions around the world, such as in Africa (Aguilar et al., 2009), America (Haylock et al., 2006; Kunkel et al., 1999a), and Asia (Klein Tank et al., 2006; Ren et al., 2011). In China, the changes in precipitation extremes in different regions have been distinct in recent decades. Generally, a decrease in extreme precipitation events has been reported in northern, central, and northeastern China, while extreme precipitation events have increased in northwestern China, southwestern China, and southern China and near the Yangtze River (Li et al., 2015; Lu et al., 2010; Wang et al., 2014; You et al., 2008; Zhai and Pan, 2003; Zhai et al., 2005). The Yangtze River and the northern part of South China experienced more severe and extreme heavy rainfall events in the 1990s (Zou and Ren, 2015). An overall increasing trend in precipitation extremes, including consecutive wet days and number of days with daily precipitation greater than 10 mm, was observed in the arid region of northwest China (Deng et al., 2014). By contrast, Zhang et al. (2015) examined changes in extreme precipitation events in the Huang-Huai-Hai River basin of China and found significant decreases in wet days, consecutive wet days, and the maximum 5-day precipitation along with a weak increasing trend for consecutive dry days. Similarly, an increasing trend in consecutive dry days was also found over the Pearl River Basin, southern China; other extreme precipitation indexes showed non-significant increasing trends (Zhao et al., 2014). The temperature extremes exhibited a consistent increasing trend, with varying intensities in diverse regions in China, and significant decreases in cold days/nights along with significant increases in warm days/nights (Deng et al., 2012, 2014; Guan et al., 2015; H. Wang et al., 2013). Both the lowest and the highest temperatures increased in recent decades, with the increasing trend of the lowest temperature being much greater than that of the highest temperature (Z. Wang et al., 2012). This resulted in a declining trend in the diurnal temperature range in China, with a rate of −0.25 °C/decade (You et al., 2013). In addition, changes in the cold and warm temperature extremes predominantly occurring in winter reflect the consistent winter warming in China (You et al., 2013). Therefore, it is more important and feasible to investigate the response of extreme climate events from a regional perspective (You et al., 2011). Regional assessments in various climates and geographic regions are needed for identifying indicators that cause environmental and other problems and for helping us obtain reliable information for rational countermeasures.

The Loess Plateau is prone to extreme climatic events, particularly floods and droughts. Most areas of the Loess Plateau have an arid or semi-arid climate. Approximately 80% of the total cultivated land area has rain-fed farming systems, and the agriculture in the Loess Plateau is greatly dependent on and sensitive to climate (Wang and Liu, 2003). Extreme events exert considerable impacts on the agriculture and soil erosion of the Loess Plateau. Because of frequent heavy rainfall in summer, steeply sloping landscapes, low vegetation cover, and highly erodible soils, the Loess Plateau has become one of the most severely eroded areas in the world. Some studies have revealed that climate change has played an important role in the agricultural and soil erosion variability in the Loess Plateau (Li et al., 2010; Wan et al., 2013; Yu et al., 2005). Loess Plateau is sensitive to global climate change; however, the changes with regard to extreme climate are not clear. Regional assessments on various climates and geographic regions are needed for understanding uncertainties in extreme events' responses to global warming. The objective of this study was to assess recent trends in extreme events in terms of precipitation and air temperature, with a particular focus on event intensity, frequency, and duration. This research will be helpful for future ecological constructions and agriculturally sustainable development.

2. Data and methods

2.1. Study area

The Loess Plateau is located in the middle reaches of the Yellow River, northern China (100°54′–114°33′ E, 33°43′–41°16′ N) (Fig. 1). It covers an area of 620,000 km^2 and is dominated by an arid and semi-arid climate. The annual average temperature ranges from 4.3 °C in the northwest to 14.3 °C in the southeast (Guo et al., 2011). The mean annual precipitation is highly heterogeneous in space, increasing from 200 mm in the northwest to 750 mm in the southeast (Li et al., 2010). The Loess Plateau is well known for its severe soil erosion, frequent floods, and serious droughts (Tang, 2004). To mitigate serious soil erosion, a series of programs for the control of soil and water loss have been conducted, particularly the "Grain to Green" program launched in 1999. Under these programs, substantial infrastructure projects have been implemented, such as large-scale reservoir development, silt dam projects, afforestation, and efforts to return steep slope cropland to forests and grasslands to increase the vegetation coverage and control water and soil losses (Xin et al., 2008).

2.2. Data sources and quality controls

We investigated 72 meteorological stations that recorded daily observations within the Loess Plateau. Of these stations, most were established in the 1950s (Table 1), but all data before 1960 were excluded in the study. Some stations, such as Dingbian, Changzhi, and Houma, were deselected because these stations were established during the study period (in 1989, 1986, and 1991, respectively). Finally, 64 out of the 72 recording stations were selected for the study based on data continuity and duration. We calculated the long-term trends for air temperature and precipitation indices based on the same number (64) of stations and the same period (1960–2013). The quality-controlled data of the average daily temperature, daily maximum temperature, daily minimum temperature, and daily precipitation were available from the National Climate Center of the China Meteorological Administration (http://www.nmic.gov.cn). The data quality control procedures detected whether the recorded data were consistent with real precipitation values (i.e., above 0 mm) and whether the daily maximum temperature exceeded the minimum temperature, among other assessments.

Homogeneity assessments of the recorded daily temperature and precipitation datasets were conducted in the Loess Plateau during the period 1960–2013. The assessment aimed to detect artificial shifts due to inevitable changes in the observing instruments, relocations, environment, and procedures during the data collection. Change-points (shifts), which are found in some data series with potential first-order autoregressive errors, can be detected and adjusted by software packages: RHtests for temperature series and RHtests-dlyprcp for precipitation series. Both software packages were developed by Wang and Feng (2013) at the Climate Research Branch of Meteorological Service of Canada (http://etccdi.pacificclimate.org/software.shtml). The

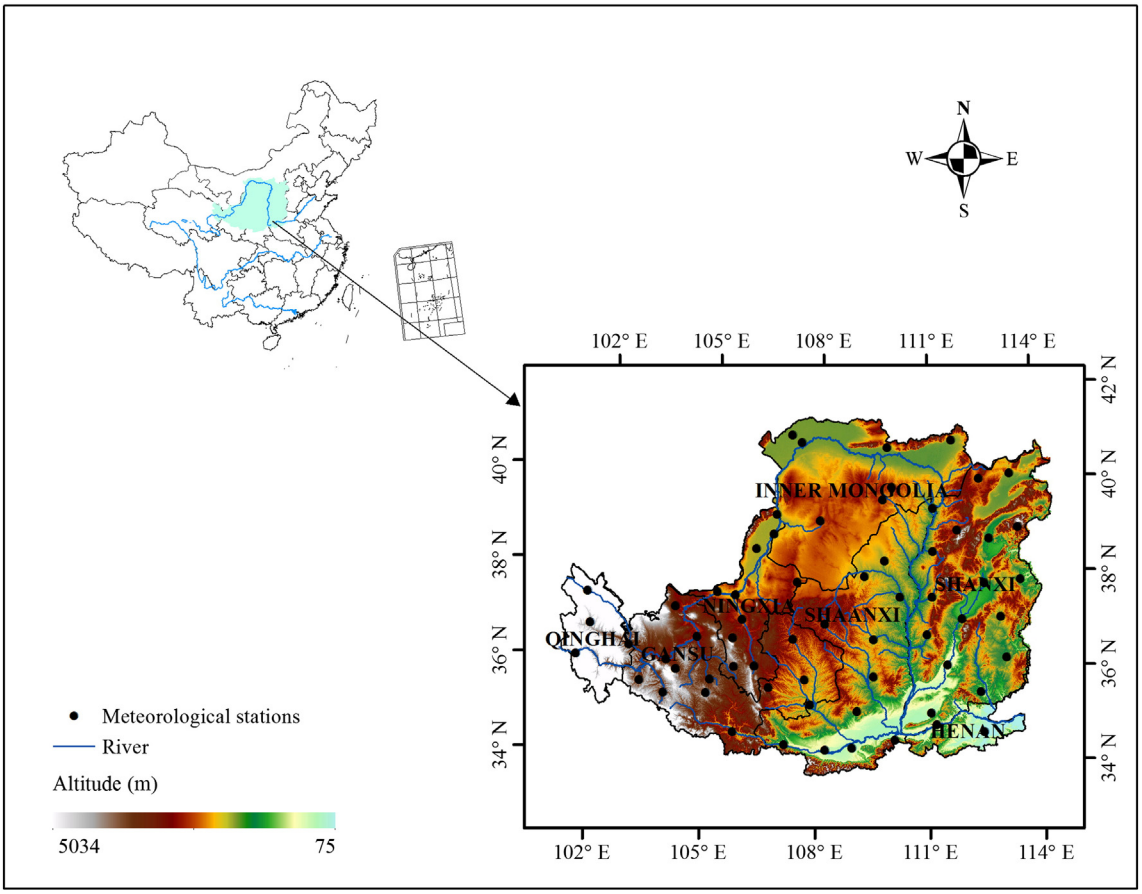

Fig. 1. Location, provincial boundaries, altitudinal variation range, and distribution of the meteorological stations in the Loess Plateau, China.

RHtests package was applied based on the penalized maximal *t* test and the penalized maximal *F* test, which are embedded in a recursive testation algorithm, with the lag-1 autocorrelation of the time series being empirically accounted for. The RHtests-dlyPrcp package is similar to the RHtests package, except that it is specifically designed for the homogenization of daily precipitation data time series. It is based on the transPMFred algorithm, which integrates a data-adaptive Box–Cox transformation procedure into the PMFred algorithm. The default parameters in both software packages were used to detect and adjust for a whole data series in each station at the 0.05 significance level. Possible single or multiple change-points in a time series can be detected in both software packages, and confirmed step changes can be adjusted (S. Wang et al., 2013). Once a possible change is identified, the metadata (including documented station relocation and instrument update) should be checked to identify any potential valid explanations. In the study, only one station with inhomogeneity in average daily temperature (Wutaishan station in Shanxi province, see Fig. 2a and b) was removed when calculating the growing season length; no change-points were found in daily maximum temperature and daily minimum temperature. Sixteen change points were detected among 64 stations in the daily precipitation series in the Loess Plateau during the period of 1960–2013; all of the change-points occurred between 1978 and 1980 (see Fig. 2c and d, Huajialing station in Gansu province). The discontinuities for all of these points resulted from the increased measuring precision of small daily precipitation amounts during the period (Wang et al., 2010). Therefore, these discontinuities will void the adjustments.

2.3. Definition of extreme indices

Extreme climate indices, including 12 extreme temperature indices and 10 extreme precipitation indices (Table 2), were used in this study. These indices can reflect the changes in intensity, frequency, and duration in of temperature and precipitation events (Alexander et al., 2006). A total of 12 extreme temperature indices and 10 extreme precipitation indices, excluding erosive rainfall, heavy rain, and rainstorm, were selected for this study as recommended by the CCl/CLIVAR/JCOMM Expert Team on Climate Change Detection and Indices (ETCCDI, http://cccma.seos.uvic.ca/ETCCDI/). Erosive rainfall has an important impact on runoff and erosion, and 12 mm daily rainfall has been used as the standard for describing erosive rainfall on the Loess Plateau (Xie et al., 2000). The criteria for heavy rain (>25 mm) and rainstorm (>50 mm) are defined by the National Climate Center of the China Meteorological Administration (http://www.nmic.gov.cn). The extreme temperature indices are grouped into three types. The absolute indices, including summer days, tropical nights, frost days, and ice days, are based on the original observational data and fixed thresholds. The relative indices, including warm days (nights) and cold days (nights), are obtained by a relative threshold (percentile) approach. The third type comprises warm and cold spell duration indicators, the diurnal temperature range, and the growing season length. Similarly, the precipitation indices are categorized into two types: precipitation intensity indices, which include simple daily intensity, maximum consecutive 5-day precipitation, and very-wet-day and extremely wet-day precipitation; and the number of days of precipitation, including consecutive wet days, consecutive dry days, erosive rainfall days, heavy precipitation days, and rainstorm days.

The regional averages were calculated as arithmetic means of the values at all selected stations in the study. We used the linear tendency estimate method to analyze trends in extreme events, and the correlations among the events based on the regional averages were analyzed using the SAS software package (SAS Institute Inc, 1990).

Table 1
List of the selected meteorological stations in the Loess Plateau, China.

No.	Station code	Station name	Province	North Latitude	East Longitude	Elevation (m)	Start time
1	52984	Linxia	Gansu	35.58	103.18	1917	1951.1
2	52986	Lintao	Gansu	35.35	103.85	1894	1951.1
3	52889	Lanzhou	Gansu	36.05	103.88	1517	1951.1
4	52797	Jingtai	Gansu	37.18	104.05	1631	1956.11
5	52983	Yuzhong	Gansu	35.87	104.15	1874	1951.1
6	52895	Jingyuan	Gansu	36.57	104.68	1398	1951.1
7	52996	Huajialing	Gansu	35.38	105.00	2451	1951.1
8	52993	Huining	Gansu	35.68	105.08	2012	1955.11
9	57006	Tianshui	Gansu	34.58	105.75	1142	1951.1
10	53915	Pingliang	Gansu	35.55	106.67	1347	1951.1
11	53821	Huanxian	Gansu	36.58	107.30	1256	1957.1
12	53923	Xifengzhen	Gansu	35.73	107.63	1421	1951.1
13	57051	Sanmenxia	Henan	34.80	111.20	410	1957.1
14	57073	Luoyang	Henan	34.63	112.47	137	1951.1
15	53420	Hangjinhouqi	Inner Mongolia	40.90	107.13	1057	1954.1
16	53513	Linhe	Inner Mongolia	40.75	107.42	1039	1956.11
17	53529	Etuokeqi	Inner Mongolia	39.10	107.98	1380	1954.10
18	53545	Yijinhuoluoqi	Inner Mongolia	39.57	109.73	1329	1958.11
19	53446	Baotou	Inner Mongolia	40.67	109.85	1067	1951.1
20	53543	Dongsheng	Inner Mongolia	39.83	109.98	1462	1956.12
21	53463	Huhehaote	Inner Mongolia	40.82	111.68	1063	1951.2
22	53704	Zhongwei	Ningxia	37.53	105.18	1226	1959.1
23	53806	Haiyuan	Ningxia	36.57	105.65	1854	1957.12
24	53705	Zhongning	Ningxia	37.48	105.68	1183	1953.1
25	53903	Xiji	Ningxia	35.97	105.72	1917	1957.2
26	53810	Tongxin	Ningxia	36.97	105.90	1339	1955.1
27	53614	Yinchuan	Ningxia	38.48	106.22	1111	1951.1
28	53817	Guyuan	Ningxia	36.00	106.27	1753	1956.10
29	53615	Taole	Ningxia	38.80	106.70	1102	1959.1
30	53519	Huinong	Ningxia	39.22	106.77	1093	1957.1
31	53723	Yanchi	Ningxia	37.80	107.38	1349	1954.1
32	52868	Guizhou	Qinghai	36.03	101.43	2237	1956.11
33	52765	Menyuan	Qinghai	37.38	101.62	7850	1956.10
34	52866	Xining	Qinghai	36.72	101.75	2295	1954.1
35	52876	Minhe	Qinghai	36.32	102.85	1814	1956.10
36	53853	Xixian	Shanxi	36.70	110.95	1053	1957.1
37	53959	Yuncheng	Shanxi	35.05	111.05	365	1956.1
38	53764	Lishi	Shanxi	37.50	111.10	951	1957.1
39	53664	Xingxian	Shanxi	38.47	111.13	1013	1955.1
40	53564	Hequ	Shanxi	39.38	111.15	862	1954.11
41	53868	Linfen	Shanxi	36.07	111.50	450	1954.1
42	53663	Wuzhai	Shanxi	38.92	111.82	1401	1957.1
43	53863	Jiexiu	Shanxi	37.03	111.92	744	1954.1
44	53975	Yangcheng	Shanxi	35.48	112.40	660	1957.1
45	53478	Youyu	Shanxi	40.00	112.45	1346	1957.1
46	53772	Taiyuan	Shanxi	37.78	112.55	778	1951.1
47	53673	Yuanping	Shanxi	38.73	112.72	828	1954.1
48	53787	Yushe	Shanxi	37.07	112.98	1041	1957.1
49	53887	Jindongnan	Shanxi	36.20	113.12	927	1953.12
50	53487	Datong	Shanxi	40.10	113.33	1067	1955.1
51	53588	Wutaishan	Shanxi	38.95	113.52	2208	1956.1
52	53782	Yangquan	Shanxi	37.85	113.55	742	1954.12
53	57016	Baoji	Shaanxi	34.35	107.13	612	1951.9
54	53929	Changwu	Shaanxi	35.20	107.80	1207	1956.9
55	53738	Wuqi	Shaanxi	36.92	108.17	1331	1956.10
56	57034	Wugong	Shaanxi	34.25	108.22	448	1954.4
57	57036	Xi'an	Shaanxi	34.30	108.93	398	1951.1
58	53947	Tongchuan	Shaanxi	35.08	109.07	979	1955.1
59	53740	Hengshan	Shaanxi	37.93	109.23	1111	1954.1
60	53845	Yan'an	Shaanxi	36.60	109.50	959	1951.1
61	53942	Luochuan	Shaanxi	35.82	109.50	1160	1954.11
62	53646	Yulin	Shaanxi	38.27	109.78	1157	1951.1
63	57046	Huashan	Shaanxi	34.48	110.08	2065	1953.1
64	53754	Suide	Shaanxi	37.50	110.22	930	1953.1

2.4. Mann–Kendall trend test

The MK test assumed that the climatic series is independent and not robust against autocorrelation, which is a major source of uncertainty in testing and interpreting trends (Li et al., 2014). To eliminate the influence of serial correlation, the "trend-free-prewhitening" procedure was employed to remove the lag-1 serial correlation from the time series (Li et al., 2014; Von Storch, 1995). A trend is considered to be statistically significant if it is significant at the 0.05 level.

2.5. Atmospheric circulation

To examine the influence of the main atmospheric circulation types on climate extremes in the Loess Plateau, a Pearson's correlation analysis

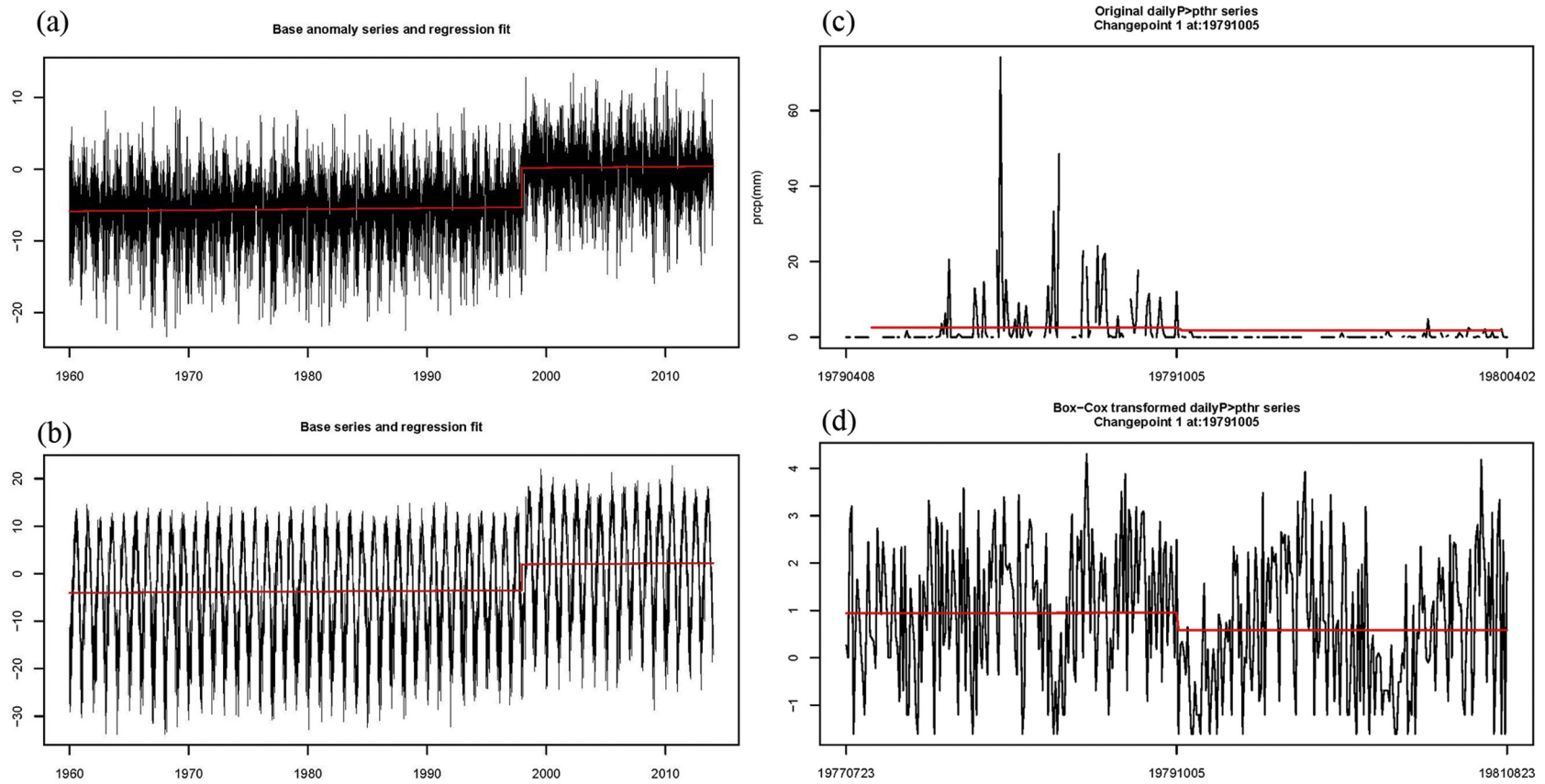

Fig. 2. Homogeneity assessment results for average daily temperatures at Wutaishan station and daily precipitation at Huajialing station, 1960–2013.

Table 2
Indices of temperature and precipitation extremes used in the study. TX denotes the daily maximum temperature, TN is the daily minimum temperature, TG is the daily mean temperature, and RR is the daily precipitation. A wet day is defined as when RR > 1 mm, and a dry day is when RR < 1 mm. The reference period for the percentiles is 1960–2010. All of the indices were calculated at the annual scale from January to December.

Index	Description	Definition	Unit
Temperature			
SU	Summer days	Annual count of days when TX >25 °C	days
TR	Tropical nights	Annual count of days when TN > 20 °C	days
FD	Frost days	Annual count of days when TN < 0 °C	days
ID	Ice days	Annual count of days when TX < 0 °C	days
TN10	Cold nights	Days when TN < 10th percentile	days
TN90	Warm nights	Days when TN > 90th percentile	days
TX10	Cold days	Days when TX < 10th percentile	days
TX90	Warm days	Days when TX > 90th percentile	days
WSDI	Warm spell duration indicator	Annual count of days with at least 6 consecutive days when TX > 90th percentile	days
CSDI	Cold spell duration indicator	Annual count of days with at least 6 consecutive days when TN < 10th percentile	days
GSL	Growing season length	Annual count between the first period of at least 6 consecutive days with TG > 5 °C and the first period after July 1 of 6 consecutive days with TG < 5 °C	days
DTR	Diurnal temperature range	Annual mean difference between TX and TN	°C
Precipitation			
PRCPTOT	Wet day precipitation	Annual total precipitation from wet days	mm
SDII	Simple daily intensity index	Average precipitation on wet days	mm/day
Rd12mm	Erosive rainfall	Annual count of days when RR > 12 mm	days
Rd25mm	Heavy rain	Annual count of days when RR > 25 mm	days
Rd50mm	Rainstorm	Annual count of days when RR > 50 mm	days
RX5day	Maximum 5-day precipitation	Annual maximum consecutive 5-day precipitation	mm
R95	Very-wet-day precipitation	Annual total precipitation when RR > 95th percentile	mm
R99	Extremely wet-day precipitation	Annual total precipitation when RR > 99th percentile	mm
CDD	Consecutive dry days	Maximum number of consecutive dry days	days
CWD	Consecutive wet days	Maximum number of consecutive wet days	days

was performed between atmospheric circulation indices and the climate extreme indices, based on the potential factors affecting the climate in Northern China (Deng et al., 2014; Dong et al., 2015; Huang et al., 2014; You et al., 2013). The selected atmospheric circulation indices included Arctic Oscillation (AO), North Atlantic Oscillation (NAO), Pacific Decadal Oscillation (PDO), South Oscillation Index (SOI), and Northern Oscillation Index (NOI), which were available from the National Oceanic and Atmospheric Administration (http://www.esrl.noaa.gov/psd/data/climateindices/list/). Another selected atmospheric circulation index used was the Western Pacific Subtropical High Intensity Index (WPSHII), which can be downloaded from the Climate Diagnostics and Prediction Division, National Climate Center, China Meteorological Administration (http://cmdp.ncc-cma.net/Monitoring/). To quantify changes in large-scale atmospheric circulation, we calculated the mean circulation composites, namely, mean geopotential height and wind fields, in summer and winter at 500 hPa for the periods 1960–1985 and 1986–2013, respectively, and subtracted the former from the latter to represent the change in circulation between the two periods. In addition, we derived the air temperature and water vapor flux divergence in the rainy season (months 6–9 in the Loess Plateau) based on the NCEP/NCAR reanalysis data between the two periods. These datasets were obtained from the National Centers for Environmental Prediction/National Center for Atmospheric Research (NCEP/NCAR) reanalysis (available from their website at http://www.cdc.noaa.gov/).

3. Results

3.1. Extreme temperature events

3.1.1. Warm extremes (SU, TR, TX90, TN90, WSDI)

The regional annual series for warm extremes in the Loess plateau during 1960–2013 are shown in Fig. 3(a, b, c, d, and e). The spatial distribution pattern of these warm extremes are demonstrated in Fig. 4(a, b, c, d and e).

Summer days (SU) and tropical nights (TR) significantly increased in the Loess plateau from 1960 to 2013. The regional trends in SU and TR were 2.76 ($P < 0.01$) and 1.24 ($P < 0.01$) days/decade, respectively (Fig. 3a and b). The sharply increased trends in SU and TR existed from 1985 to 2000 at the rates of 0.83 and 0.53 days/year, respectively (Fig. 3a and b). For SU and TR, 73% and 58% of stations, respectively, show significant increasing trends (Fig. 4a and b). For SU, the areas that experienced significant increases mainly occurred in western, northern, southern, and some scattered eastern Loess Plateau (Fig. 4a). For TR, the significant increases over time were concentrated in northwestern, central, and eastern plateau (Fig. 4b).

Over 1960–2013, the regionally averaged occurrence of warm days (TX90) and nights (TN90) significantly increased by 2.60 ($P = 0.0003$) and 3.41 ($P < 0.01$) days/decade, respectively (Fig. 3c and d). Similarly, the sharply increasing trends in TX90 and TN90 were also found between 1985 and 2000. The 57% of stations with significant increasing trends for TX90 mainly occurred in western, northwestern, and a few stations in the eastern Loess Plateau (Fig. 4c). For TN90, approximately 78% of the stations, covered nearly the entire plateau, showed significant increases in which the local trends exceeded 6 days/decade (Fig. 4d).

The warm spell duration indicator (WSDI) increased by 0.68 days/decade ($P = 0.0041$) over the most recent five decades (Fig. 3e), only 33% of stations in some regions significantly increased over the past 50 years within a rate of 2–4 days/decade (Fig. 4e).

3.1.2. Cold extremes (FD, ID, TX10, TN10, CSDI)

The regional changes in cold extremes in the Loess Plateau during 1960–2013 are shown in a similar way in Fig. 3(f, g, h, i, and j). The spatial variability in these cold indicators is demonstrated in Fig. 4(f, g, h, i, and j).

In contrast to warm extremes, frost days (FD) and ice days (ID) significantly decreased in the Loess Plateau during the past 50 years. The regional trends in FD and ID were −3.22 ($P < 0.01$) and −2.21 ($P = 0.0028$) days/decade in 1960–2013, respectively (Fig. 3f and g). The sharply decreasing trend in FD and ID occurred from 1970 to 2000 of the study period at the rates of −3.7 and −4.9 days/decade, respectively (Fig. 3f and g). FD in most of the Loess Plateau (83% of stations) significantly decreased over time, mainly ranging from −2 to −6 days/decade (Fig. 4f). ID with downward trends (−2 and −4 days/decade) were mainly located in the central and eastern regions of the plateau (Fig. 4g).

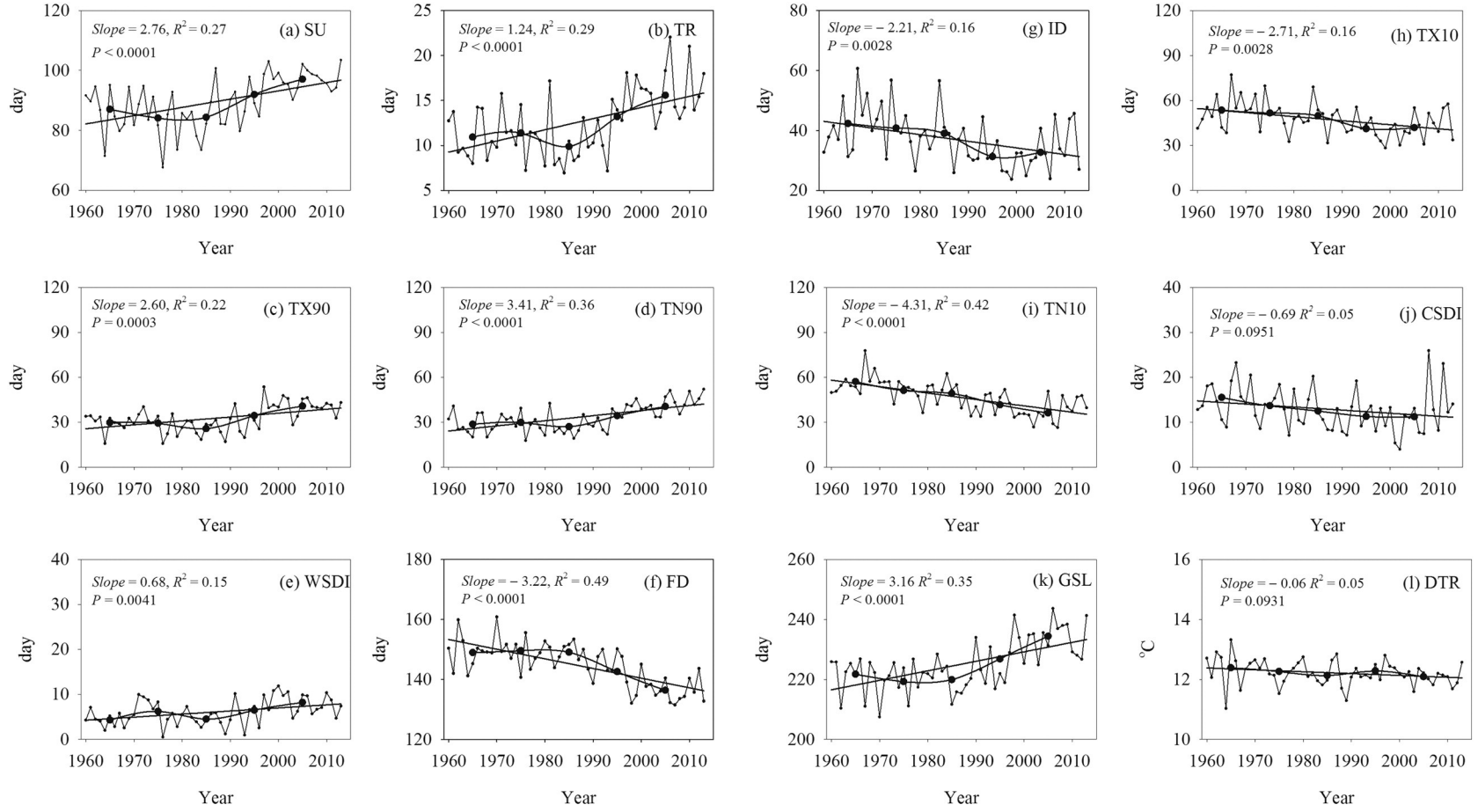

Fig. 3. Regionally averaged series for indices of the annual and decadal extreme temperature events in the Loess Plateau from 1960 to 2013. The straight line represents the linear regression for the datasets during 1960–2013.

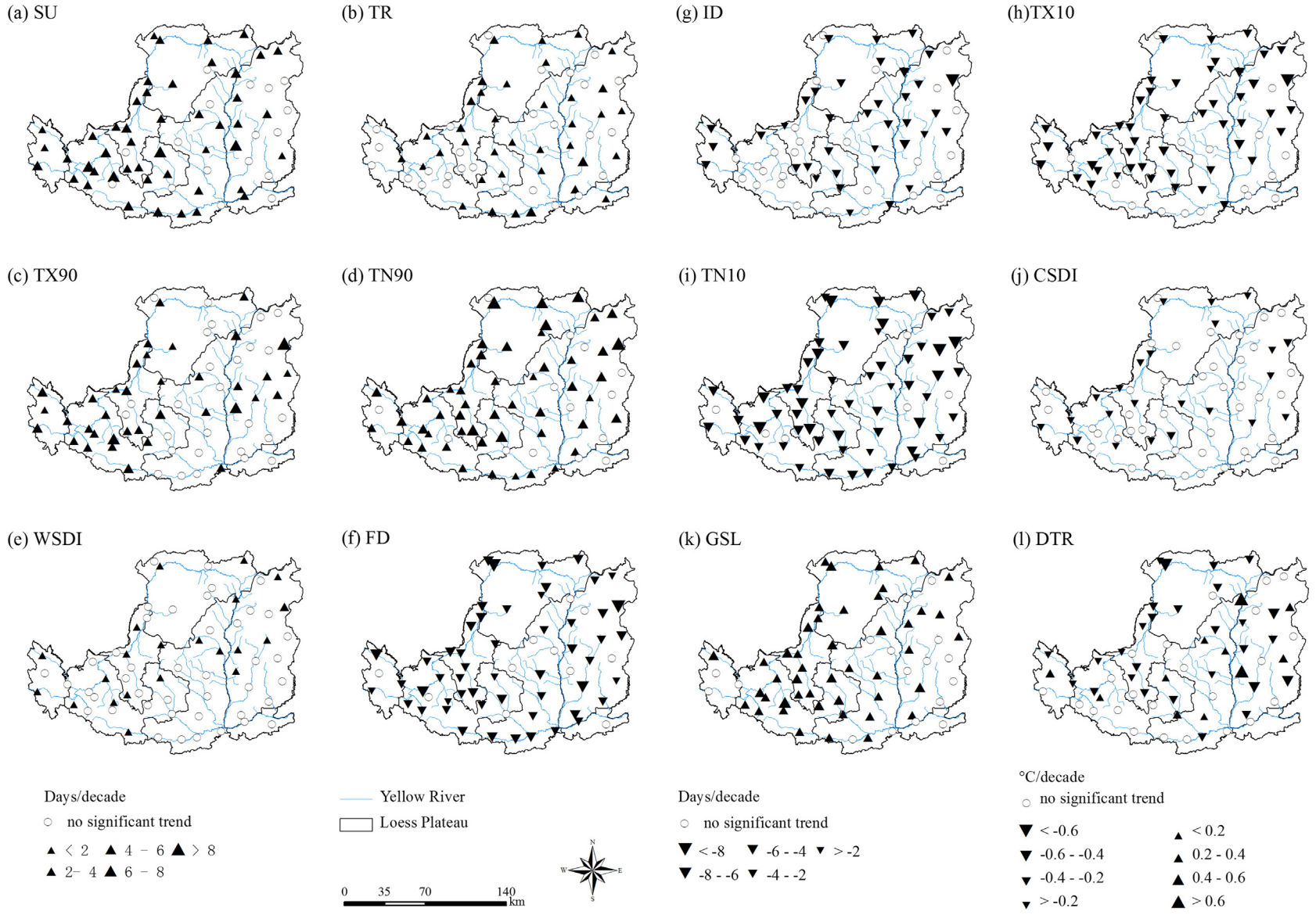

Fig. 4. Spatial pattern of the decadal trends in the indices of extreme temperature events over the Loess Plateau during the most recent five decades. The significantly positive and negative trends are shown as up and down strangles at the 0.05 level (MK test), and circles with hollow filled represented no significant trends.

The relative indices of the cold extreme temperature events obviously vary across the Loess Plateau (Figs. 3h and i, Fig. 4h and i). Over 1960–2013, the occurrence of cold days (TX10) and nights (TN10) significantly decreased by −2.71 ($P = 0.0028$) and −4.31 ($P < 0.01$) days/decade, respectively (Fig. 3h and i). For TX10 and TN10, approximately 75% and 89% of stations significantly decreased during the past 50 years, which covered nearly in entire regions of the Loess Plateau (Fig. 4h and i). The significant decrease in TX10 in most areas varied from −2 to −6 days/decade (Fig. 4h), while most of the stations with significant decreases in TN10 exhibited at local rates between −4 and −8 days/decade (Fig. 4i).

The cold spell duration indicator (CSDI) decreased by −0.69 days/decade ($P = 0.0951$) in the Loess Plateau during the 1960–2013; however, it was not significant at the 0.05 level (Fig. 3j). 36% of stations significantly decreased over the past 50 years within a rate of −2 to −4 days/decade (Fig. 4j), which mainly located in western plateau and some scattered eastern areas.

3.1.3. Growing season length and diurnal temperature range

The growing season (GSL) in the Loess Plateau was lengthened at a rate of 3.16 days/decade ($P < 0.01$), particularly in 1985–2005 at a rate of 9.4 days/decade (Fig. 3k). For GSL, 73% of stations had significant positive trends, mainly increased between 2 and 6 days/decade (Fig. 4k). The average regional diurnal temperature range (DTR) declined at a rate of −0.06 °C/decade ($P = 0.0931$), but it did not change significantly at the 0.05 level (Fig. 3l). About 19% of stations in DTR show significant increasing trends; however, most of stations (45%) on the Loess Plateau in DTR significant decreased (Fig. 4l).

On average, the trend magnitudes for cold extremes were larger than those for warm extremes. For example, the changes of regional trends in FD (3.22 days/decade) and ID (2.21 days/decade) were higher than SU (2.76 days/decade) and TR (1.24 days/decade) from 1960 to 2013. Similarly, the trend magnitudes in cold nights (TN10, 4.31 days/decade) are more than that of warm day (TX90, 2.60 days/decade).

3.1.4. Correlation coefficients of temperature indices

The correlation coefficients of the temperature indices are listed in Table 3. The warm and cold extremes, except for diurnal temperature range ($R = 0.10$), were highly correlated with the mean annual temperature, with correlation coefficients higher than 0.5 ($P < 0.01$). The warm temperature indices were positively correlated with the mean temperature, and the correlation coefficients ranged from 0.59 to 0.77. Summer days had the strongest correlations with the mean temperature (i.e., a correlation of 0.77). Negative correlations between the mean temperature and cold indicators were also significant, and cold nights exhibited the highest correlation (R = -0.85). In addition, there were high correlations among the warm indices and among cold indices. For example, summer days were highly related to warm days, and the highest correlation coefficient existed between tropical nights and warm nights. Similar characteristics were also found for the cold indices.

3.2. Extreme precipitation events

3.2.1. Regional and spatial trends in extreme precipitation events

The regional, annual series of extreme precipitation indices are shown in Fig. 5. The spatial distribution of the trends in these indices is shown in Fig. 6.

The annual total precipitation (PRCPTOT) showed no obvious trends ($P = 0.7828$) in the Loess Plateau over the 53-year period (Fig. 5a). The distribution of PRCPTOT focused between 6 and 9 month in the Loess Plateau, and the precipitation in 6–9 months accounted for 74% of PRCPTOT (Fig. 5b). The proportion of precipitation in 6–9 months exhibited a decrease at a rate of −0.83%/decade ($P = 0.1304$) from 1960 to 2013 (Fig. 5c). Similarly, the proportion of erosive rainfall (R12mm), heavy rain (R25mm), and rainstorm (R50mm) exhibited decreases over time; however, these changes were not significant at the 0.05 level (Fig. 5d, e and f). The occurrences of erosive rainfall (Rd12mm), heavy rain (Rd25mm), and rainstorm (Rd50mm) also exhibited no significant changes over time (Fig. 5g, h, and i). Spatially, 97% in Rd12mm, 95% in Rd25mm, and 98% in Rd50mm of stations had no significant trends at the 0.05 level (Fig. 6d, e, and f).

The daily rainfall intensity (SDII) exhibited a significant decrease of −0.14 mm/day/decade ($P = 0.0158$) over 1960–2013, particularly, a sharp decrease was found from 1970 to 1985 of the study periods (Fig. 5j). Approximately 22% of stations in SDII exhibited significant decreasing trends, mainly occurred in southern and eastern Loess Plateau (Fig. 6a). The maximum consecutive 5-day precipitation (RX5day) and very-wet-day (R95) and extremely wet-day (R99) precipitation had no statistically significant trends over the five decades (Fig. 5k, l and m). The regionally averaged consecutive dry days (CCD) significantly increased from 1960 to 2013 at a rate of 1.96 days/decade ($P = 0.0001$), practically, a sharp increase in CCD existed between 1970 and 1990 (Fig. 5n). The 56% of stations with significantly increasing trends in CCD mainly located in central and southern parts of the Loess Plateau (Fig. 6h). In contrast, the consecutive wet days (CWD) showed no obvious trends over the 53-year period ($P = 0.4106$) (Fig. 5o).

3.2.2. Correlation coefficients of precipitation indices

The annual total precipitation was well correlated (at the 0.01 significance level) with the extreme precipitation, excluding the consecutive dry days ($R = -0.02$) (Table 4). The correlation coefficients between the annual total precipitation and the extreme precipitation indices,

Table 3
Correlation coefficients of extreme temperature indices in the Loess Plateau between 1960 and 2013.

	TG	SU	TR	TX90	TN90	WSDI	GSL	FD	ID	TX10	TN10	CSDI	DTR
TG	1												
SU	0.77**	1											
TR	0.66**	0.57**	1										
TX90	0.74**	0.83**	0.75**	1									
TN90	0.69**	0.59**	0.95**	0.73**	1								
WSDI	0.59**	0.63**	0.72**	0.84**	0.66**	1							
GSL	0.76**	0.52**	0.50**	0.53**	0.56**	0.34**	1						
FD	−0.81**	−0.54**	−0.54**	−0.52**	−0.62**	−0.36**	−0.86**	1					
ID	−0.74**	−0.40**	−0.33**	−0.41**	−0.33**	−0.30*	−0.38**	0.40**	1				
TX10	−0.75**	−0.40**	−0.33**	−0.39**	−0.33**	−0.30*	−0.43**	0.43**	0.97**	1			
TN10	−0.85**	−0.47**	−0.43**	−0.42**	−0.45**	−0.34**	−0.58**	0.64**	0.73**	0.80**	1		
CSDI	−0.51**	−0.24	−0.34**	−0.32*	−0.30*	−0.30*	−0.17	0.20	0.57**	0.60**	0.62**	1	
DTR	0.10	0.39*	−0.08	0.30*	−0.17	0.17	−0.06	0.29*	−0.32**	−0.31*	0.06	−0.08	1

* Significant at the 0.05 level.
** Significant at the 0.01 level

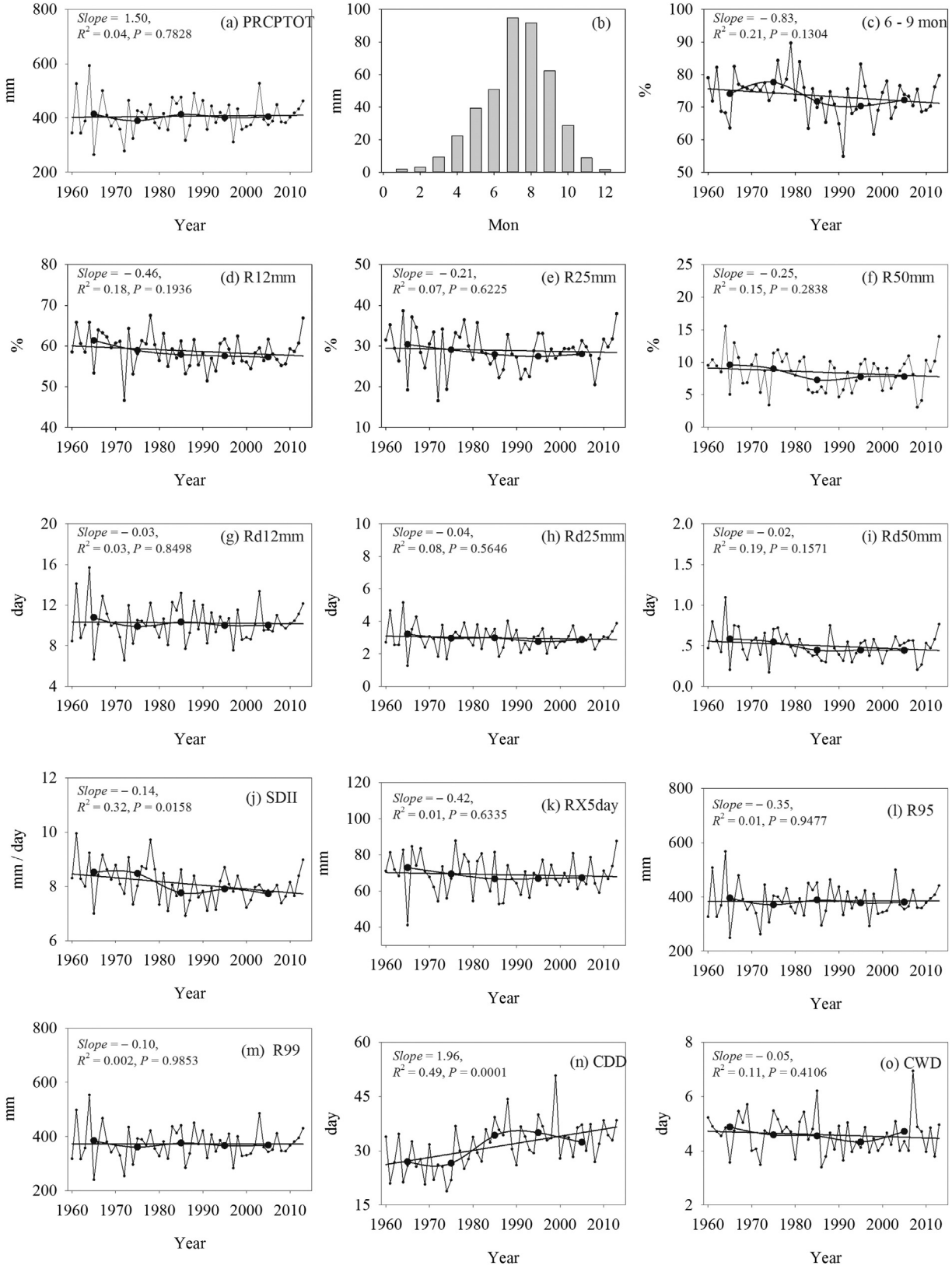

Fig. 5. Regionally averaged series for indices of annual and decadal extreme precipitation events in the Loess Plateau from 1960 to 2013. The straight line represents the linear regression for the datasets during 1960–2013.

including the very-wet-day precipitation, extremely wet-day precipitation, erosive rainfall days, and heavy rain days exceeded 0.9, and the other correlations exceeded 0.49. In addition, statistically significant correlations existed among the extreme precipitation indices.

4. Discussion

Global warming is exacerbating and triggering particular climate extremes, including decreasing the frequency of cold days and cold nights

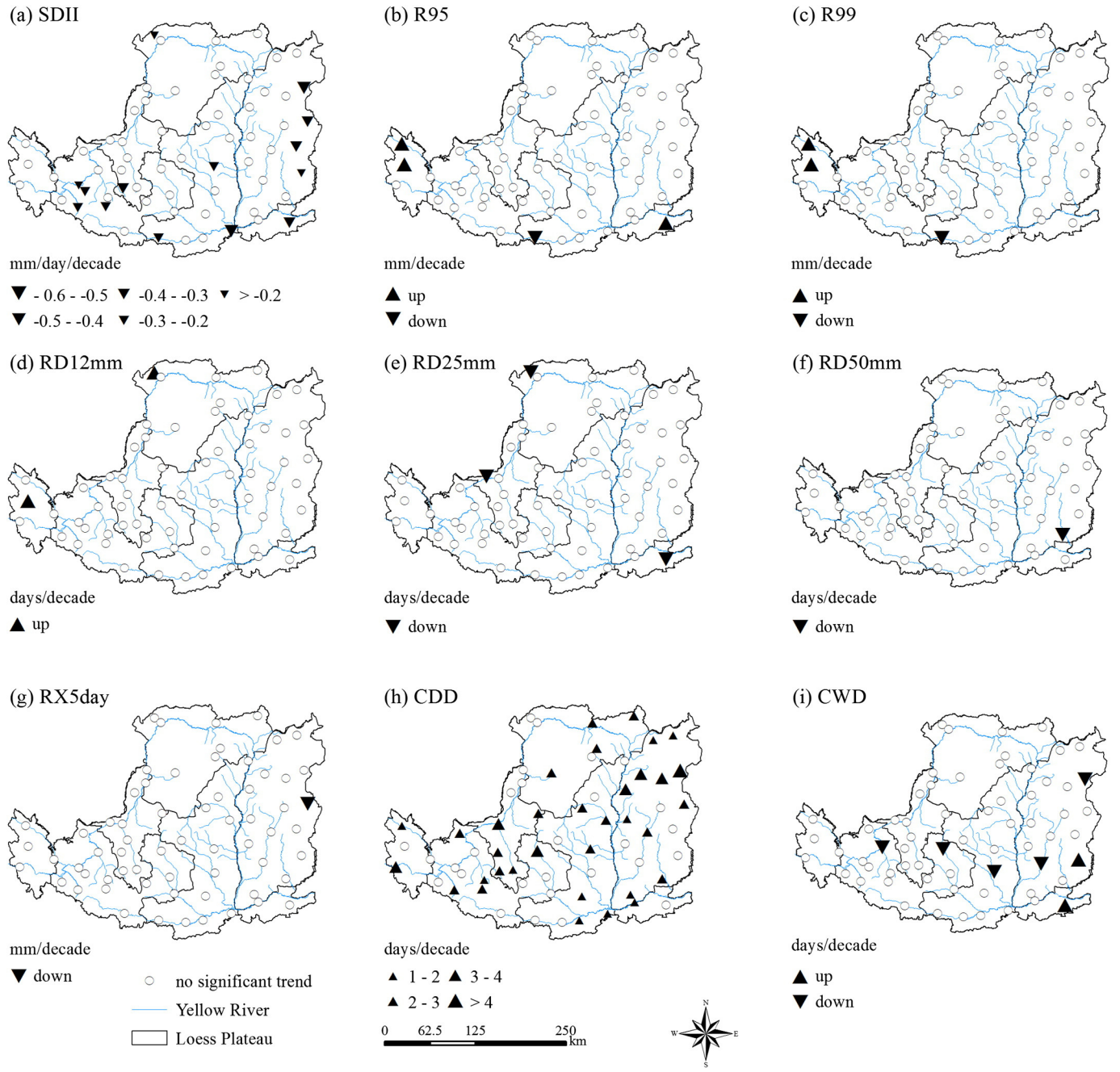

Fig. 6. Spatial pattern of decadal trends in indices of extreme precipitation events in the Loess Plateau during the most recent five decades. The significantly positive and negative trends are shown as up and down strangles at the 0.05 level (MK test), and circles with hollow filled represented no significant trends.

and increasing the frequency of warm days and warm nights (IPCC, 2007). In addition, numerous simulation experiments of future climate events also indicate that a warming climate results in many extreme climate events (Kharin et al., 2007; H. Wang et al., 2012; Zwiers et al., 2013). In this study, cold-temperature extremes significantly decreased, while warm-temperature extremes and the growing season significantly increased in the Loess Plateau during the most recent five decades, particularly, the rapid warming trends occurred in almost the entire Loess Plateau during the periods between 1985 and 2000 (Figs. 3 and 4). Our results confirmed that extreme temperature events in the Loess Plateau were strongly consistent with other similar studies in many regions regarding their response to recent global warming. For example, Alexander et al. (2006) found that cold nights decreased and warm nights increased at approximately 70% of locations worldwide over 50 years. Similar work has been implemented in the Europe and in the Asia-Pacific region (Choi et al., 2009; Klein Tank and Können, 2003). Both studies have achieved similar conclusions after analyzing the variations in extreme temperature events. Extreme temperature events have also been studied by many researchers in China (Table 5). The patterns of these events are consistent with the general regional warming trends found in Xinjiang (Northwest China) during 1960–2009 (B. Wang et al., 2013), in the Tibetan Plateau during 1973–2011 (S. Wang et al., 2013), in far-west China during 1960–2004 (Zhang et al., 2009), and around the Yangtze River during 1962–2011 (Su et al., 2006; Wang et al., 2014). The extremes are also consistent with the warming at the national scale (Xu et al., 2011; Zhai et al., 2005; Zhang et al., 2011). The trend magnitudes for warm and cold extremes in the Loess Plateau were lower than that in Xinjiang (northwest China)

Table 4
Correlation coefficients of the extreme precipitation indices in the Loess Plateau between 1960 and 2013.

	PRCPTOT	SDII	Rd12mm	Rd25mm	Rd50mm	RX5day	R95	R99	CDD	CWD
PRCPTOT	1									
SDII	0.63**	1								
Rd12mm	0.97**	0.70**	1							
Rd25mm	0.91**	0.80**	0.90**	1						
Rd50mm	0.69**	0.75**	0.65**	0.82**	1					
RX5day	0.65**	0.72**	0.65**	0.73**	0.71**	1				
R95	0.99**	0.66**	0.98**	0.92**	0.71**	0.66**	1			
R99	0.99**	0.67**	0.98**	0.92**	0.71**	0.66**	0.99**	1		
CDD	−0.02	−0.13	−0.08	−0.05	−0.03	0.05	−0.04	−0.04	1	
CWD	0.49**	0.38**	0.50**	0.43**	0.30*	0.64**	0.49**	0.49**	−0.14	1

* Significant at the 0.05 level.
** Significant at the 0.01 level.

and Tibetan Plateau (western China), but greater than that in Yangzi River (central and south China), Yunnan–Guizhou plateau (southwestern China), and national scale of China (Table 5). Furthermore, our study revealed that the magnitudes of the trends in cold extremes, which predominantly occurred in winter, were larger than those in warm extremes in the Loess Plateau (Figs. 3 and 4), which indicated that winter temperatures were warming more quickly than summer temperatures.

The warming trends in the temperature extremes in the Loess Plateau, primarily in the cold extremes, were closely related with the atmospheric circulation index, WPSHII (Fig. 7a), based on a Pearson's correlation analysis (Table 6). The WPSHII, which accounts for approximately one quarter of the Northern Hemispheric surface in summer, represents a large-scale anticyclonic circulation identified as one of the dominant components of the East Asian summer monsoon climate system (Huang et al., 2014). In the study, the WPSHII is positively correlated with warm extremes, including SU ($R = 0.35$, $P < 0.01$), TR, TX90, TN90, and WSDI, and is significantly negatively correlated with cold extremes, including FD ($R = -0.27$, $P < 0.05$), ID ($R = -0.46$, $P < 0.01$), TX10 ($R = -0.46$, $P < 0.01$), TN10 ($R = -0.46$, $P < 0.01$), and CSDI ($R = -0.27$, $P < 0.05$). Furthermore, the WPSHII is associated with the warming and drying trend through not only the extension of the growing season length (GSL, $R = 0.27$, $P < 0.05$) but also an increase in the consecutive dry days ($R = 0.34$, $P < 0.01$). These results indicate that the WPSHII strongly influences warm/cold extremes and contributes significantly to climate changes in the Loess Plateau. In addition to the WPSHII, the AO (Fig. 7b) has been shown to be less sensitive to the changes in climate extremes in the Loess Plateau (Table 6). The AO is a major controlling factor in Northern Hemisphere climate variability and is also correlated with the strength of the East Asian winter monsoon and the Siberian higher pressure system (You et al., 2013). The AO index is negatively correlated with cold extremes and has a significant influence on ID ($R = -0.31$, $P < 0.05$). Meanwhile, the AO index is also significantly related with DTR, with a correlation value of -0.51 ($P < 0.01$), which is consistent with the asymmetrical warming in China (You et al., 2013). A possible reason for this correlation is the reduction of the intensity of the Asian winter monsoon. To investigate the role of circulation change in the extreme trends, we also created circulation composite maps from the NCEP/NCAR reanalysis in summer and winter at 500 hPa between two halves of the study period (1960–1985 and 1986–2013). The increased geopotential height over Mongolia is consistent with rapid warming in warm extremes, and the flow pattern tended to prevent any northward transportation of water vapor, which increased the occurrence of drought and resulted in the continuous increment of air temperature in northern China (Fig. 8a). In winter, anticyclone circulation (centered on 40°N and 120°E) has

Table 5
Trends of temperature and precipitation extremes from this study and other works in China.

Index	This study	Global	China	Northwest China (Xinjiang)	Western China (Tibetan Plateau)	Northeast China (Songhua River)	Central and South China (Yangzi River)	Southwestern China (Yunnan–Guizhou plateau)
Temperature								
SU	**2.76**	–	1.18	**2.14**	0.42	–	**0.29**	–
TR	**1.24**	–	–	**1.71**	–	–	**0.18**	–
TX90	**2.60**	**0.89**	0.62	**3.59**	**3.43**	–	**0.22**	**0.22**
TN90	**3.41**	**1.58**	**1.75**	**6.23**	**4.00**	–	**0.29**	**0.36**
WSDI	**0.68**	–	–	**0.88**	**3.31**	–	**0.08**	–
FD	**−3.22**	–	**−3.73**	**−3.69**	**−5.68**	–	**−0.33**	**−0.29**
ID	**−2.21**	–	–	**−1.61**	**−7.74**	–	**−0.05**	−0.09
TX10	**−2.71**	**−0.62**	−0.47	**−2.60**	**−2.84**	–	**−0.08**	**−0.13**
TN10	**−4.31**	**−1.26**	**−2.06**	**−6.57**	**−4.92**	–	**−0.28**	**−0.37**
CSDI	−0.69	–	–	**−1.27**	**−2.55**	–	**−0.07**	–
GSL	**3.16**	–	**3.04**	**2.74**	**4.35**	–	**0.23**	**0.12**
DTR	−0.06	**−0.08**	**−0.18**	**−0.26**	**−0.20**	–	**−0.01**	**−0.18**
Precipitation								
PRCPTOT	1.50	**10.59**	3.21	–	0.47	1.65	1.9	0.03
SDII	**−0.14**	0.05	0.06	0.04	0.014	**−0.02**	**0.05**	0.03
R95	−0.35	**4.07**	**4.06**	**6.28**	0.48	1.37	2.7	0.04
R99	−0.10	–	–	**3.26**	0.41	1.28	1.1	**0.05**
RX5day	−0.42	0.55	1.90	**0.85**	1.25	0.13	–	0.03
CDD	**1.96**	−0.55	−1.22	−0.02	0.52	**0.22**	–	−0.05
CWD	−0.05	–	–	0.05	0.17	0.00	–	**−0.08**

Notes: Data sources and time period: Global during 1951–2003 (Alexander et al., 2006); China during 1961–2003 (You et al., 2011); Xinjiang, Northwest China during 1960–2009 (Wang et al., 2013a); Tibetan Plateau, Western China during 1973–2011 (Wang et al., 2013c); Songhua River Basin, Northeast China during 1960–2013 (Song et al., 2015); Yangzi River Basin, temperature extremes during 1962–2011 (Wang et al., 2014) and precipitation extremes during 1960–2005 (Zhang et al., 2008); Yunnan–Guizhou plateau, including the Sichuan, Yunnan, and Guizhou Provinces, the Tibet Autonomous Region and Chongqing Municipality, Southwestern China during 1961–2008 (Li et al., 2012). Values for trends significant at the 0.05 level are set bold face.

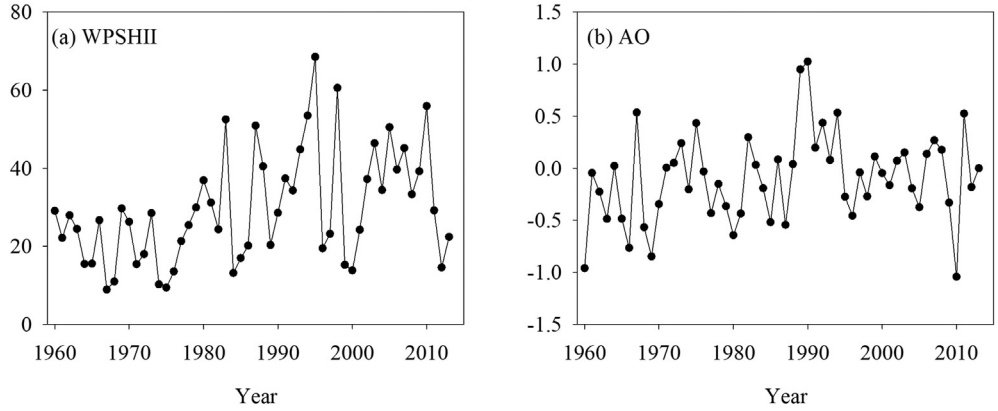

Fig. 7. Time series of WPSHII (a) and AO (b) indices in the Loess Plateau during the period 1960–2013.

been enhanced since 1986, and the southwesterly wind in northern Mongolia has been strengthened, which has weakened the southern extent of the winter monsoon, limited its southward extension, and reduced incursions of colder air in northern China (Fig. 8b). Cold temperature extremes were significantly decreased, which is consistent with the trend of increased air temperature at 500 hPa in winter (Fig. 8c). These findings explain why the cold temperatures extremes have greatly decreased in the Loess Plateau. The changes in the daytime and nighttime temperatures are asymmetrical, and the diurnal temperature range is decreasing due to global warming.

Anomalous variability in climate extreme events is always associated with frequent occurrences of extreme droughts/floods and heat waves/cold surges, which have substantial and direct influences on society and the ecological environment (Kunkel et al., 1999b; Rosenzweig et al., 2001). The correlations between climatic indicators and vegetation have been observed for a long time; thus, complex relationships exist between vegetation growth and climate variables. In the Loess Plateau, both of the ecological effects of climate warming on the environment were observed (Hao et al., 2012; Huang et al., 2009; Xin et al., 2008). Our study indicates that the frequency and intensity in warm temperature extremes were greatly enhanced in the Loess Plateau in the most recent 50 years, particularly in 1985–2000 (Fig. 3a, b, c, d, and e). Increased temperatures and extreme heat might dry the soil and inhibit vegetation growth. However, the vegetation growing periods have been lengthened in response to global warming during the past three decades (Figs. 3k and 4k). Previous studies have confirmed that the increased temperatures favor vegetation growth in spring and autumn because of the longer growing period (Sun et al., 2015; Xin et al., 2008). Some studies have also focused on the adverse impacts on the ecological environment due to climate warming. For example, the degraded land in the upstream area of the Yellow River is increasing at an annual rate of 1.83% (Hao et al., 2012). Water discharge in the Yellow River has experienced a steady decrease since the 1970s and has resulted in the severe deterioration of alpine meadows (Huang et al., 2009).

Assessments of climates and extreme events are helpful for further understanding the influences of climatic extremes on soil erosion in the Loess Plateau. In our study, the annual total precipitation showed no obvious trends ($P = 0.7828$) in the Loess Plateau (Fig. 5a); however, the daily rainfall intensity exhibited significant decreases (−0.14 mm/day/decade, $P = 0.0158$) (Fig. 5j). Furthermore, the proportions of erosive rainfall ($P = 0.1936$) and rainstorm ($P = 0.2838$) exhibited decreases in the Loess Plateau over the 53-year period (Fig. 5d and f), although there were no significances at the 0.05 level. Simultaneously, soil erosion and sediment transported to the Yellow River has been substantially reduced, which is likely associated with the deceasing daily rainfall intensity, erosive rainfall, and rainstorm (Miao et al., 2010; Sun et al., 2014; Xin et al., 2011). In addition, consecutive dry days significantly increased at a rate of 1.96 days/decade ($P < 0.01$), practically, a sharp increase existed between 1970 and 1990 (Fig. 5n). In summer, the enhanced high pressure pattern over the Eurasian continent suggested a weaker eastern Asian summer monsoon in 1986–2013 compared with 1960–1985 (Fig. 8a). The northeasterly wind in northern and eastern China strengthened (Fig. 8a) and in turn weakened the northern and eastern extent of the westerly jet stream and any southwesterly flow from the ocean, causing a short rainy season and a drying trend in northern China (You et al., 2011). This may explain the deceasing trends of proportions of precipitation based on intensity and increases in consecutive dry days, given the difficulty that the monsoon would have faced in penetrating into this region. Although the annual precipitation in the Loess Plateau did not show a significant decreasing trend, consecutive dry days significantly increased since 1980 (Fig. 5n). The changes in water vapor divergence for the rainy season (June to September) exhibited a regional increasing drying trend in the Loess Plateau during the period 1986–2013 (Fig. 8d), which was consistent with the variation in consecutive dry days in the Loess Plateau.

Table 6
Pearson's correlation coefficients between the extreme indices and atmospheric circulation indices in the Loess Plateau during the period 1960–2013. Notes: Arctic Oscillation (AO), North Atlantic Oscillation (NAO), Pacific Decadal Oscillation (PDO), South Oscillation Index (SOI), Northern Oscillation Index (NOI), and Western Pacific Subtropical High Intensity Index (WPSHII).

Index	AO	NAO	PDO	SOI	NOI	WPSHII
SU	−0.07	−0.13	−0.13	0.10	0.07	0.35**
TR	−0.01	−0.22	−0.23	0.24	0.24	0.21
TX90	−0.02	−0.16	−0.23	0.03	0.13	0.19
TN90	0.07	−0.17	−0.28*	0.27*	0.30*	0.24
WSDI	0.08	−0.02	−0.27*	0.14	0.11	0.13
GSL	0.08	−0.14	−0.12	−0.01	0.14	0.27*
FD	−0.31*	−0.03	−0.11	−0.04	−0.23	−0.27*
ID	−0.01	0.01	−0.21	0.25	0.22	−0.46**
TX10	−0.04	0.04	−0.20	0.23	0.20	−0.46**
TN10	−0.23	−0.10	−0.08	0.12	−0.01	−0.46**
CSDI	−0.04	−0.15	−0.23	0.31*	0.21	−0.27*
DTR	−0.51**	−0.24	0.10	−0.37*	−0.35*	0.08
PCPTOT	0.26*	0.07	0.01	0.18	0.20	0.05
SDII	0.12	−0.16	−0.17	0.17	0.18	−0.07
Rd12mm	0.17	−0.01	−0.01	0.17	0.19	−0.05
Rd25mm	0.11	−0.03	−0.08	0.25	0.25	−0.01
Rd50mm	0.09	−0.07	−0.20	0.24	0.29	−0.09
RX5day	−0.04	−0.14	−0.23	0.19	0.23	−0.07
R95	0.25	0.06	−0.01	0.18	0.21	0.05
R99	0.23	0.06	−0.01	0.19	0.21	0.04
CDD	−0.13	−0.05	0.29*	−0.06	−0.10	0.34**
CWD	0.06	0.01	−0.11	0.21	0.28*	−0.14

* Significant at the 0.05 level.
** Significant at the 0.01 level.

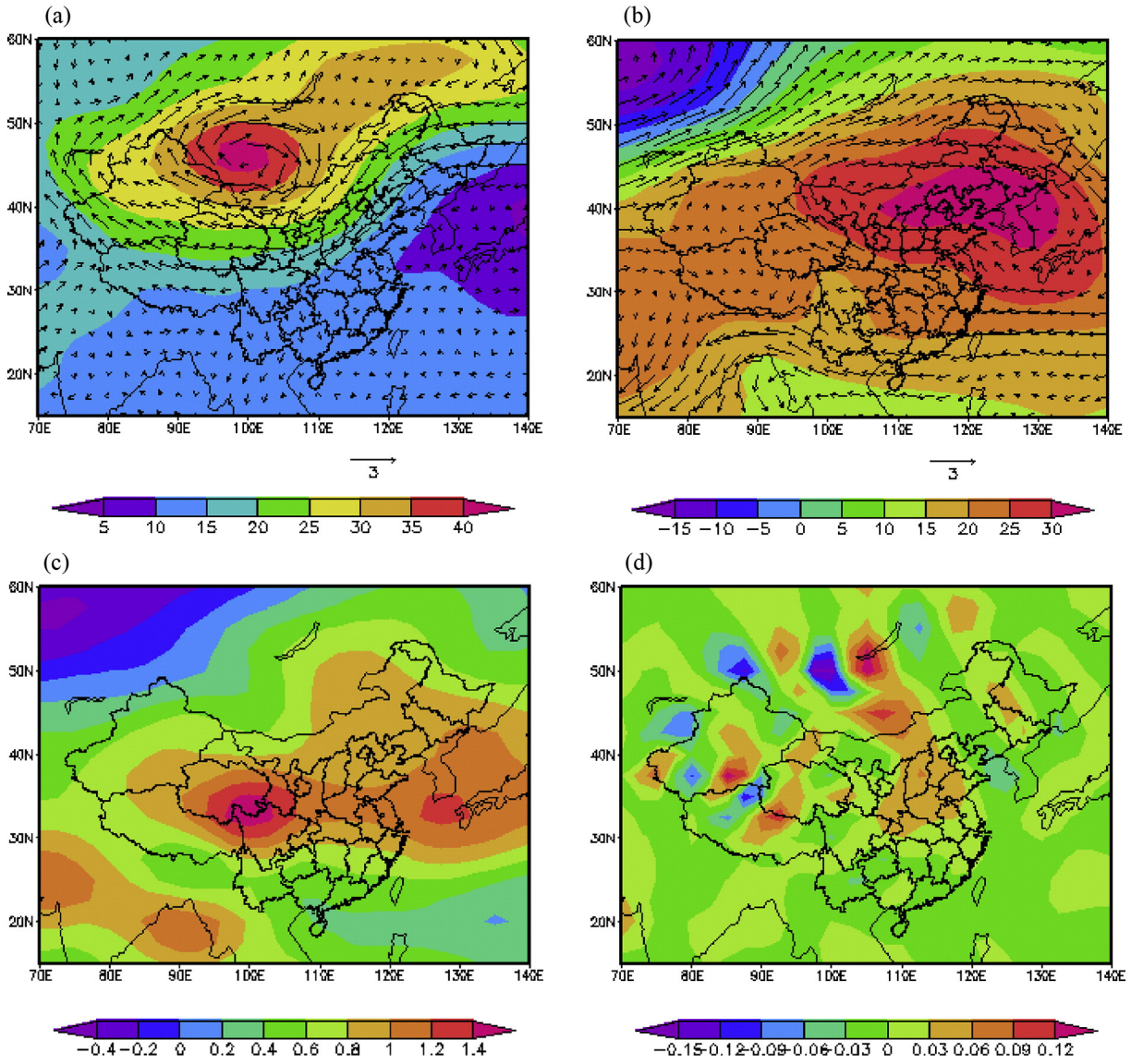

Fig. 8. Differences of geopotential height and wind speed in summer (a) and winter (b), air temperature in winter (c), and water vapor divergence (d) for the wet season (June to September) at 500 hPa between 1986–2013 and 1960–1985.

5. Conclusions

We used 12 extreme temperature and 10 extreme precipitation indices of magnitude, intensity, and persistence to quantify the extreme climate changes in the Loess Plateau. The regionally averaged trends and the spatial changes in these indices were analyzed at 64 meteorological stations during 1960–2013. All of the temperature-based indices showed consistent warming trends. The cold indices, including cold days and nights, ice days, and frost days significantly decreased in the Loess Plateau during the past five decades. Over the same period, the warm indices, including warm days and nights, summer days, tropical nights, warm spell duration, and growing season length, significantly increased. Furthermore, the magnitudes of the trends in the cold extremes are larger than those in the warm extremes. Extreme warm events in most regions tended to increase, while extreme cold events tended to decrease in the Loess Plateau. With the exception of the diurnal temperature range, the indices strongly correlate with the annual mean temperature. The average daily rainfall intensity exhibited a significant regional decrease during 1960–2013, while consecutive dry days exhibited a significant increase. The other indices of precipitation extremes, including the maximum consecutive 5-day precipitation, very-wet-day and extremely wet-day precipitation, consecutive wet days, and days with varying precipitation intensities exhibited no significant trends during 1960–2013. The variations in the precipitation indices are closely related to the changes in the annual total precipitation in the Loess Plateau. Large-scale atmospheric circulation indices, such as WPSHII and AO, strongly influence warm/cold extremes and contribute significantly to climate changes in the Loess Plateau. The strengthening anticyclone circulation, increasing geopotential height, and rapid warming have contributed to the changes in climate extremes in the Loess Plateau.

Acknowledgments

This research was supported by the Governmental public industry research special funds for projects (201501049), the National Natural Science Foundation of China (41501293, 41501022), and the Natural Science Foundation of Shaanxi Province (2015JQ4112).

References

Aguilar, E., Aziz Barry, A., Brunet, M., Ekang, L., Fernandes, A., Massoukina, M., Mbah, J., Mhanda, A., Do Nascimento, D., Peterson, T., 2009. Changes in temperature and precipitation extremes in western central Africa, Guinea Conakry, and Zimbabwe, 1955–2006. J. Geophys. Res. Atmos. (1984–2012) 114 (D2).

Alexander, L., Zhang, X., Peterson, T., Caesar, J., Gleason, B., Klein Tank, A., Haylock, M., Collins, D., Trewin, B., Rahimzadeh, F., 2006. Global observed changes in daily climate extremes of temperature and precipitation. J. Geophys. Res. Atmos. (1984–2012) 111 (D5).

Choi, G., Collins, D., Ren, G., Trewin, B., Baldi, M., Fukuda, Y., Afzaal, M., Pianmana, T., Gomboluudev, P., Huong, P.T.T., 2009. Changes in means and extreme events of temperature and precipitation in the Asia-Pacific Network region, 1955–2007. Int. J. Climatol. 29 (13), 1906–1925.

Deng, H., Zhao, F., Zhao, X., 2012. Changes of extreme temperature events in Three Gorges area, China. Environ. Earth Sci. 66 (7), 1783–1790.

Deng, H., Chen, Y., Shi, X., Li, W., Wang, H., Zhang, S., Fang, G., 2014. Dynamics of temperature and precipitation extremes and their spatial variation in the arid region of northwest China. Atmos. Res. 138, 346–355.

Dong, B., Sutton, R., Highwood, E., Wilcox, L., 2015. Preferred response of the East Asian summer monsoon to local and non-local anthropogenic sulphur dioxide emissions. Clim. Dyn. 1–19.

Fankhauser, S., 1995. Valuing climate change: the economics of the greenhouse. Routledge, Earthscan Publications Limited, (London).

Guan, Y., Zhang, X., Zheng, F., Wang, B., 2015. Trends and variability of daily temperature extremes during 1960–2012 in the Yangtze River Basin, China. Glob. Planet. Chang. 124, 79–94.

Guo, R., Li, F., He, W., Yang, S., Sun, G., 2011. Spatial and temporal variability of annual precipitation during 1958-2007 in Loess Plateau, China. Computer and Computing Technologies in Agriculture IV. Springer, pp. 551–560.

Hao, F., Zhang, X., Ouyang, W., Skidmore, A.K., Toxopeus, A., 2012. Vegetation NDVI linked to temperature and precipitation in the upper catchments of Yellow River. Environ. Model. Assess. 17 (4), 389–398.

Haylock, M.R., Peterson, T., Alves, L., Ambrizzi, T., Anunciação, Y., Baez, J., Barros, V., Berlato, M., Bidegain, M., Coronel, G., 2006. Trends in total and extreme South American rainfall in 1960–2000 and links with sea surface temperature. J. Clim. 19 (8), 1490–1512.

Huang, Y., Cai, J., Yin, H., Cai, M., 2009. Correlation of precipitation to temperature variation in the Huanghe River (Yellow River) basin during 1957–2006. J. Hydrol. 372 (1), 1–8.

Huang, Y., Wang, H., Fan, K., Gao, Y., 2014. The western Pacific subtropical high after the 1970s: westward or eastward shift? Clim. Dyn. 44 (7-8), 2035–2047.

IPCC, 2007. Summary for Policymakers of Climate Change 2007: The Physical Science Basis. Contribution of Working Group I to the Fourth Assessment Report of the Intergovernmental Panel on Climate Change. Cambridge University Press, Cambridge, UK.

Kharin, V.V., Zwiers, F.W., Zhang, X., Hegerl, G.C., 2007. Changes in temperature and precipitation extremes in the IPCC ensemble of global coupled model simulations. J. Clim. 20 (8), 1419–1444.

Klein Tank, A., Können, G., 2003. Trends in indices of daily temperature and precipitation extremes in Europe, 1946–99. J. Clim. 16 (22), 3665–3680.

Klein Tank, A., Peterson, T., Quadir, D., Dorji, S., Zou, X., Tang, H., Santhosh, K., Joshi, U., Jaswal, A., Kolli, R., 2006. Changes in daily temperature and precipitation extremes in central and south Asia. J. Geophys. Res. Atmos. (1984–2012) 111 (D16).

Kunkel, K.E., Andsager, K., Easterling, D.R., 1999a. Long-term trends in extreme precipitation events over the conterminous United States and Canada. J. Clim. 12 (8), 2515–2527.

Kunkel, K.E., Pielke Jr., R.A., Changnon, S.A., 1999b. Temporal fluctuations in weather and climate extremes that cause economic and human health impacts: a review. Bull. Am. Meteorol. Soc. 80 (6), 1077–1098.

Li, Z., Liu, W., Zhang, X., Zheng, F., 2009. Impacts of land use change and climate variability on hydrology in an agricultural catchment on the Loess Plateau of China. J. Hydrol. 377 (1), 35–42.

Li, Z., Zheng, F., Liu, W., Flanagan, D.C., 2010. Spatial distribution and temporal trends of extreme temperature and precipitation events on the Loess Plateau of China during 1961–2007. Quat. Int. 226 (1), 92–100.

Li, Z., He, Y., Wang, P., Theakstone, W.H., An, W., Wang, X., Lu, A., Zhang, W., Cao, W., 2012. Changes of daily climate extremes in southwestern China during 1961–2008. Glob. Planet. Chang. 80, 255–272.

Li, F., Zhang, G., Xu, Y.J., 2014. Spatiotemporal variability of climate and streamflow in the Songhua River. Basin, northeast China. J. Hydrol. 514, 53–64.

Li, Y.G., He, D.M., Hu, J.M., Cao, J., 2015. Variability of extreme precipitation over Yunnan Province, China 1960–2012. Int. J. Climatol. 35 (2), 245–258.

Liu, W., Zhang, M., Wang, S., Wang, B., Li, F., Che, Y., 2013. Changes in precipitation extremes over Shaanxi Province, northwestern China, during 1960–2011. Quat. Int. 313–314, 118–129.

Lu, H., He, H., Chen, S., 2010. Spatiotemporal variation of extreme precipitation frequency in summer over South China in 1961–2008. Chin. J. Ecol. 6, 1213–1220.

Marengo, J., Jones, R., Alves, L.M., Valverde, M., 2009. Future change of temperature and precipitation extremes in South America as derived from the PRECIS regional climate modeling system. Int. J. Climatol. 29 (15), 2241–2255.

Meehl, G.A., Karl, T., Easterling, D.R., Changnon, S., Pielke Jr., R., Changnon, D., Evans, J., Groisman, P.Y., Knutson, T.R., Kunkel, K.E., 2000. An introduction to trends in extreme weather and climate events: observations, socioeconomic impacts, terrestrial ecological impacts, and model projections*. Bull. Am. Meteorol. Soc. 81 (3), 413–416.

Miao, C., Ni, J., Borthwick, A.G., 2010. Recent changes of water discharge and sediment load in the Yellow River basin, China. Prog. Phys. Geogr. 34 (4), 541–561.

Mu, X., Basang, C., Zhang, L., Gao, P., Wang, F., Zhang, X., 2007. Impact of soil conservation measures on runoff and sediment in Hekou-Longmen region of the Yellow River. J. Sediment. Res. 2, 36–41.

Ouyang, W., Hao, F., Skidmore, A.K., Toxopeus, A., 2010. Soil erosion and sediment yield and their relationships with vegetation cover in upper stream of the Yellow River. Sci. Total Environ. 409 (2), 396–403.

Ren, G., Guan, Z., Shao, X., Gong, D., 2011. Change in climatic extremes over mainland China. Clim. Res. 50 (1-2), 105–111.

Rosenzweig, C., Iglesias, A., Yang, X., Epstein, P.R., Chivian, E., 2001. Climate change and extreme weather events; implications for food production, plant diseases, and pests. Glob. Chang. Hum. Health 2 (2), 90–104.

SAS Institute Inc, 1990. SAS/STAT User's Guide, Version 6, 4th ed., vol. 2. SAS Inst., Cary, NC. SAS Institute.

Song, X., Song, S., Sun, W., Mu, X., Wang, S., Li, J., Li, Y., 2015. Recent changes in extreme precipitation and drought over the Songhua River Basin, China, during 1960–2013. Atmos. Res. 157, 137–152.

Su, B., Jiang, T., Jin, W., 2006. Recent trends in observed temperature and precipitation extremes in the Yangtze River basin, China. Theor. Appl. Climatol. 83 (1-4), 139–151.

Sun, W.Y., Shao, Q.Q., Liu, J.Y., Zhai, J., 2014. Assessing the effects of land use and topography on soil erosion on the Loess Plateau in China. Catena 121, 151–163.

Sun, W., Song, X., Mu, X., Gao, P., Wang, F., Zhao, G., 2015. Spatiotemporal vegetation cover variations associated with climate change and ecological restoration in the Loess Plateau. Agric. For. Meteorol. 209–210, 87–99.

Tang, K.L., 2004. Soil and Water Conservation in China. Chinese Science Press, Beijing.

Von Storch, V.H., 1995. Misuses of statistical analysis in climate researchvon. In: Storch, H., Navarra, A. (Eds.), Analysis of Climate Variability: Applications of Statistical Techniques. Springer-Verlag, Berlin, pp. 11–26.

Wan, L., Zhang, X., Ma, Q., Zhang, J., Ma, T., Sun, Y., 2013. Spatiotemporal characteristics of precipitation and extreme events on the Loess Plateau of China between 1957 and 2009. Hydrol. Process. 28 (18), 3650–3656.

Wang, X.L., Feng, Y., 2013. RHtestsV4 User Manual. Climate Research Division Atmospheric Science and Technology Directorate Science and Technology Branch, Environment Canada, Toronto, Ontario, Canada.

Wang, F., Liu, W., 2003. Preliminary study of climate vulnerability of agro-production in the Loess Plateau. Clim. Environ. Res. 8 (1), 91–100.

Wang, X.L., Chen, H., Wu, Y., Feng, Y., Pu, Q., 2010. New techniques for the detection and adjustment of shifts in daily precipitation data series. J. Appl. Meteorol. Climatol. 49 (12), 2416–2436.

Wang, H., Sun, J., Chen, H., Zhu, Y., Zhang, Y., Jiang, D., Lang, X., Fan, K., Yu, E., Yang, S., 2012a. Extreme climate in China: facts, simulation and projection. Meteorol. Z. 21 (3), 279–304.

Wang, Z., Ding, Y., Zhang, Q., Song, Y., 2012b. Changing trends of daily temperature extremes with different intensities in China. Acta Meteorol. Sin. 26 (4), 399–409.

Wang, B., Zhang, M., Wei, J., Wang, S., Li, S., Ma, Q., Li, X., Pan, S., 2013a. Changes in extreme events of temperature and precipitation over Xinjiang, northwest China, during 1960–2009. Quat. Int. 298, 141–151.

Wang, H., Chen, Y., Chen, Z., Li, W., 2013b. Changes in annual and seasonal temperature extremes in the arid region of China, 1960–2010. Nat. Hazards 65 (3), 1913–1930.

Wang, S., Zhang, M., Wang, B., Sun, M., Li, X., 2013c. Recent changes in daily extremes of temperature and precipitation over the western Tibetan Plateau, 1973–2011. Quat. Int. 313, 110–117.

Wang, Q., Zhang, M., Wang, S., Ma, Q., Sun, M., 2014. Changes in temperature extremes in the Yangtze River Basin, 1962–2011. J. Geogr. Sci. 24 (1), 59–75.

Xie, Y., Liu, B.Y., Zhang, W.B., 2000. Study on standard of erosive rainfall. J. Soil Water Conserv. 14 (4), 6–11 (in Chinese).

Xin, Z., Xu, J., Zheng, W., 2008. Spatiotemporal variations of vegetation cover on the Chinese Loess Plateau (1981–2006): impacts of climate changes and human activities. Sci. China Ser. D Earth Sci. 51 (1), 67–78.

Xin, Z., Yu, X., Lu, X., 2011. Factors controlling sediment yield in China's Loess Plateau. Earth Surf. Process. Landf. 36 (6), 816–826.

Xu, X., Du, Y., Tang, J., Wang, Y., 2011. Variations of temperature and precipitation extremes in recent two decades over China. Atmos. Res. 101 (1), 143–154.

You, Q., Kang, S., Pepin, N., Yan, Y., 2008. Relationship between trends in temperature extremes and elevation in the eastern and central Tibetan Plateau, 1961–2005. Geophys. Res. Lett. 35 (4).

You, Q., Kang, S., Aguilar, E., Pepin, N., Flügel, W.-A., Yan, Y., Xu, Y., Zhang, Y., Huang, J., 2011. Changes in daily climate extremes in China and their connection to the large scale atmospheric circulation during 1961–2003. Clim. Dyn. 36 (11-12), 2399–2417.

You, Q., Ren, G., Fraedrich, K., Kang, S., Ren, Y., Wang, P., 2013. Winter temperature extremes in China and their possible causes. Int. J. Climatol. 33 (6), 1444–1455.

Yu, L., Cao, M., Li, K., 2005. An overview of assessment of ecosystem vulnerability to climate change. Prog. Geogr. 1, 61–69.

Zhai, P., Pan, X., 2003. Change in extreme temperature and precipitation over northern China during the second half of the 20th century. Acta Geograph. Sin. 58 (S1), 1–10.

Zhai, P., Zhang, X., Wan, H., Pan, X., 2005. Trends in total precipitation and frequency of daily precipitation extremes over China. J. Clim. 18 (7), 1096–1108.

Zhang, Q., Xu, C., Zhang, Z., Chen, Y.D., Liu, C., Lin, H., 2008. Spatial and temporal variability of precipitation maxima during 1960–2005 in the Yangtze River basin and possible association with large-scale circulation. J. Hydrol. 353 (3), 215–227.

Zhang, Q., Xu, C., Zhang, Z., Chen, Y.D., 2009. Changes of temperature extremes for 1960–2004 in Far-West China. Stoch. Env. Res. Risk A. 23 (6), 721–735.

Zhang, Q., Li, J., Chen, Y.D., Chen, X., 2011. Observed changes of temperature extremes during 1960–2005 in China: natural or human-induced variations? Theor. Appl. Climatol. 106 (3-4), 417–431.

Zhang, D., Yan, D., Wang, Y., Lu, F., Wu, D., 2015. Changes in extreme precipitation in the Huang-Huai-Hai River basin of China during 1960–2010. Theor. Appl. Climatol. 120 (1-2), 195–209.
Zhao, Y., Zou, X., Cao, L., Xu, X., 2014. Changes in precipitation extremes over the Pearl River Basin, southern China, during 1960–2012. Quat. Int. 333, 26–39.
Zou, X.K., Ren, F.M., 2015. Changes in regional heavy rainfall events in China during 1961–2012. Adv. Atmos. Sci. 32 (5), 704–714.
Zwiers, F.W., Alexander, L.V., Hegerl, G.C., Knutson, T.R., Kossin, J.P., Naveau, P., Nicholls, N., Schär, C., Seneviratne, S.I., Zhang, X., 2013. Climate extremes: challenges in estimating and understanding recent changes in the frequency and intensity of extreme climate and weather events. Climate Science for Serving Society. Springer, pp. 339–389.